Hindawi
International Journal of Antennas and Propagation
Volume 2020, Article ID 6056712, 7 pages
https://doi.org/10.1155/2020/6056712

Research Article

Propagation of Electromagnetic Wave into an Illuminated Polysilicon PV Cell

Vinci de Dieu Bokoyo Barandja,[1,2] Bernard Zouma,[1] Auguste Oscar Mackpayen,[3] Martial Zoungrana,[1] Issa Zerbo ,[1] and Dieudonné Joseph Bathiebo[1]

[1]*Laboratory of Thermal and Renewable Energies, Department of Physics, Unit of Training and Research in Pure and Applied Sciences, University Joseph KI-ZERBO, Ouagadougou 03 BP 7021, Burkina Faso*
[2]*Department of Physics, University of Bangui, Bangui BP 908, Central African Republic*
[3]*Ecole Normale Supérieure, University of Bangui, Bangui BP 908, Central African Republic*

Correspondence should be addressed to Issa Zerbo; iszerbo@gmail.com

Received 15 October 2019; Revised 17 December 2019; Accepted 2 January 2020; Published 30 January 2020

Academic Editor: Mauro Parise

The increasing cohabitation between telecommunication antennas generating electromagnetic waves and solar panels poses the problem of interaction between these radio waves and solar cells. In order to study the effect of radio waves on the performance of a polycrystalline silicon solar cell in a three-dimensional approach, it is necessary to assess the attenuation of the radio wave in the illuminated polysilicon grain and also to find the expressions of its components. This work investigated the attenuation of radio waves into a polycrystalline silicon grain by analyzing, firstly, the behaviour of the penetration length of the radio waves into the polysilicon grain and secondly, the behaviour of the attenuation factor. The propagation of the radio waves into the polycrystalline silicon grain can be considered without attenuation that can be neglected.

1. Introduction

The interaction between illuminated cells that behave as an electric conductor and radio waves causes the attenuation of these waves in the solar cells and the difficulty of determining the expressions of the electric and magnetic fields of the waves. In a previous work, we investigated the attenuation of radio waves through a polysilicon solar cell illuminated by a monochromatic light by analyzing the behaviour of the attenuation factor and by considering the size of the grain and the incident light wavelength [1].

In this present work, we studied the attenuation of radio waves in a polysilicon solar cell which is illuminated with multispectral light. The study considered the size of the grain and the recombination velocity at grain boundaries and analyzed the behaviour of the penetration length as well as one of the attenuation factors.

2. Theoretical Background

The propagation of the electromagnetic field generated by radio waves into a polysilicon grain illuminated by multispectral light is illustrated in Figure 1. The polysilicon grain is isolated from a polycrystalline back surface field silicon PV cell with the n^+–p–p^+ structure. The following assumptions were made in this study:

(i) The grain has a parallelepipedic form with the same electronic and electrical parameters like the solar cell [2, 3].

(ii) The recombination velocity S_{gb} at grain boundaries is constant and independent of illumination, while the grain boundaries are perpendicular to the junction [2].

(iii) The low doped p-type base is quasi-neutral so that the crystalline electric field in the base of the solar cell can be neglected [4].

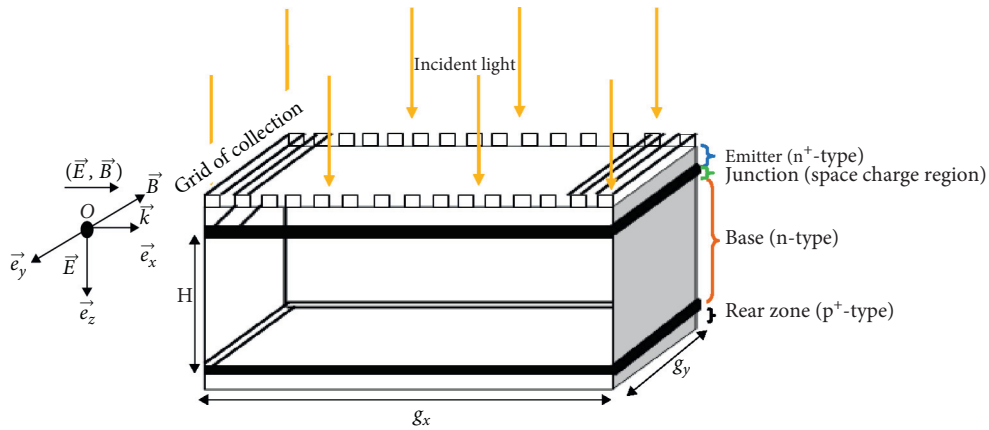

Figure 1: Illuminated polysilicon grain under the electromagnetic wave.

(iv) The concentration of electrons photogenerated in the p-type base is so lower than the doping density of the base so that the analysis was developed in the assumption of low-level injection.

(v) The electromagnetic wave is a radio wave which meets the polysilicon grain in the z-depth base region such as $0 < z < H$ [1].

(vi) The base thickness of the polysilicon grain is $H = 0.03$ cm and the electron parameters are $S_b = 104$ cm s^{-1}, $S_{gb} = 103$ cm s^{-1}, $L_n = 0.015$ cm, and $D_n = 26$ cm^2 s^{-1}

(vii) The theoretical efficiency of the PV cell, calculated using previous values and grain size $g = g_x = g_y = 0.01$ cm, is 15.70%.

In Figure 1, the electromagnetic wave travelling into the polysilicon solar grain is progressive, plane, and monochromatic. It is polarized linearly in the (Oz) direction, and it propagates in the increasing x direction [5].

In free space, the expressions of the electric and magnetic fields are given by equations (1) and (2), respectively [5]:

$$\underline{\vec{E}} = E_0 \vec{e}_z \exp j(kx - \omega t), \tag{1}$$

$$\underline{\vec{B}} = -B_0 \vec{e}_y \exp j(kx - \omega t). \tag{2}$$

The electric and magnetic field expressions in the polysilicon grain are given by equations (3) and (4), respectively [1]:

$$\underline{\vec{E}}(x,t) = E_0 \vec{e}_z \exp\left(\frac{-x}{l_p}\right) \exp j(\omega\sqrt{\varepsilon\mu}\, x - \omega t), \tag{3}$$

$$\underline{\vec{B}}(x,t) = -\frac{\sqrt{\mu_r \varepsilon_r} E_0}{c} \vec{e}_y \exp\left(\frac{-x}{l_p}\right) \exp j(\omega\sqrt{\varepsilon\mu}\, x - \omega t), \tag{4}$$

where $\ell_p = (2/\gamma)\sqrt{\varepsilon/\mu}$ is the penetration length of the radio waves in the polysilicon grain.

The penetration length is the distance on which the magnitude of the electromagnetic wave is divided by exp (1) and the value of the magnitude of the electric field is $0.367E_0$:

$$E_0 \exp\left(\frac{-x}{l_p}\right) = \frac{E_0}{\exp(1)} \Longrightarrow \exp\left(\frac{-x}{l_p}\right) = \exp(-1) \Longrightarrow x = l_p. \tag{5}$$

The characteristic penetration length l_p depends on the physical properties of the polysilicon grain which are the electric permittivity ε and the magnetic permeability μ. It also depends on the conductivity $\gamma = e\mu_n \delta(x, y, z)$ of the illuminated polysilicon grain in absence of the electromagnetic wave.

$\delta(x, y, z)$ is the density of electrons photogenerated in the base of the illuminated polysilicon grain in absence of electromagnetic wave. To find the expression of the density of electrons photogenerated by multispectral illumination in the base of the polysilicon grain, one must replace the monochromatic generation rate of excess minority carriers (electrons-holes pairs) by the multispectral one in the expression given by Ouedraogo et al. [1].

The quantity $\exp(-x/l_p)$ is the attenuation factor that characterizes the behaviour of the electric and magnetic fields of the radio waves into the polysilicon grain.

When an electromagnetic radiation arrives on a material, some wavelengths are absorbed. The part of the electromagnetic radiation which is absorbed modifies the energy of the material.

In fact, an electromagnetic wave carries energy during its propagation and the maximum value of this energy for radio waves is about 10^{-6} eV. Thus, radio waves which carry low quantity of energy cannot ionize atoms of silicon because their energy ($\approx 10^{-6}$ eV) is inferior to the bandgap energy E_g of silicon, which is 1.12 eV at 300 K and 1.16 eV at 0 K.

When radio waves during their propagation meet the polycrystalline silicon grain, there is interaction between the radio waves and the excess minority carriers photogenerated (electrons) in the base of the polysilicon solar cell, resulting in an attenuation of the amplitude of the electric and magnetic fields related to these radio waves. This attenuation is due to the absorption of energy by the conductive matter which is the illuminated polysilicon grain. Furthermore, this interaction manifests itself by an exchange of energy between the radio waves and the photogenerated electrons in the base of the polycrystalline silicon solar cell.

Thus, the interaction between the radio waves and the polysilicon grain cannot generates electrons-holes pairs, but it is the origin of an exchange of energy with electrons photogenerated by the multispectral light.

However, the photogenerated electrons in the base can be accelerated by the electric field of the radio waves and collide with the tied electrons of atoms of silicon to create electrons-holes pairs resulting in an avalanche effect.

3. Results and Discussion

For investigating the propagation of radio waves through the polysilicon grain, this study analyzed in the first time the behaviour of the penetration length of the radio waves into the polysilicon grain and secondly the behaviour of the attenuation factor. This was done considering the size of the grain and the recombination velocity at grain boundaries.

3.1. Penetration Length of the Radio Waves. An investigation of the attenuation of the radio waves by analyzing the characteristic length of the penetration can be done considering three cases.

If $l_p = g$ with $g = g_x = g_y$, the amplitude of the electric field is $E_0 \exp(-1) = 0.367E_0$ and the attenuation of the electric field is $|E_0 \exp(-1) - E_0| = E_0|\exp(-1) - 1| = 0.633E_0$ or an attenuation rate of about 63.3%.

If $l_p \ll g$, $E_0 \exp(-g/l_p) \ll E_0 \exp(-1)$, $E_0 \exp(-g/l_p) \ll 0.367E_0$, and the attenuation of the electric field is superior to $0.633E_0|E_0 \exp(-g/l_p) - E_0| \gg 0.633E_0$, leading to an attenuation rate superior to 63.3%, $|E_0 \exp(-g/l_p) - E_0|/E_0 \cdot 100 \gg 0.633E_0/E_0 \cdot 100$.

One can conclude that the electromagnetic wave is greatly vanished in the polycrystalline silicon grain.

If $l_p \gg g$, $E_0 \exp(-g/l_p) \gg E_0 \exp(-1)$, $E_0 \exp(-g/l_p) \gg 0.367E_0$, and the attenuation of the electric field is $|E_0 \exp(-g/l_p) - E_0| \ll 0.633E_0$, resulting in an attenuation rate inferior to 63.3%, $|E_0 \exp(-g/l_p) - E_0|/E_0 \cdot 100 \ll 0.633E_0/E_0 \cdot 100$.

In this case, the radio waves cross the polysilicon grain with a low attenuation. The more the penetration length of the radio waves l_p is, the less the radio waves attenuation is because there is no interaction between the radio waves and the polysilicon grain.

In this study, the classification of different grains according to their size is presented in Table 1 [6].

3.2. Effect of the Grain Size. Figures 2(a) and 2(b) plot the penetration length of the radio waves in the polysilicon grain against the base depth for different grain sizes in short circuit and open circuit conditions.

Curves of Figures 2(a) and 2(b) overlap, and this shows that irrespective of the grain size of the solar cell, the characteristic length of the penetration has the same value in the base.

In the short circuit, Figure 2(a) shows three characteristics regions: the first region is closed to the junction where the characteristic length of the penetration decreases strongly; in the second region, inside the base, where the penetration length of the radio waves is constant with the lowest value. In the third regionn closed near the rear side of the solar cell, the characteristic length of the penetration increases.

The vicinity of the junction and the rear side of the solar cell are the regions where the quantity of electrons photogenerated is the lowest. Indeed, the excess minority carriers (electrons) are either accelerated by the electric field of the junction to participate in the photocurrent or they are submitted to the phenomenon of recombination in the rear side of the solar cell.

In the short circuit, the electrons closed to the junction cross it to create the short circuit photocurrent so that the quantity of electrons at the junction is very low resulting in a very high value of the characteristic length of the penetration.

Table 2 gives the behaviour of radio waves near the junction in short circuit condition.

Inside the base of the polysilicon grain, the quantity of electrons photogenerated is the highest resulting in a lowest value of the penetration length. This lowest value is about 8 cm which corresponds to a multicrystalline grain.

The behaviour of the electromagnetic wave inside the base of the polycrystalline silicon grain in the short circuit condition is given in Table 3.

In the open circuit, curves in Figure 2(b) increase from the junction to the rear side of the polysilicon grain but the values of the characteristic length of the penetration is smaller than those of the short circuit condition. In fact, in the open circuit, the quantity of excess minority carriers photogenerated is higher than the one in the short circuit and this quantity decreases from the junction to the rear side of the polysilicon grain. The characteristic length of the penetration is being inversely proportional to the density of electrons photogenerated so the penetration length increases from the junction ($l_p = 0.691$ cm) to the rear side of the polysilicon grain ($l_p = 12$ cm).

The lowest value of the characteristic length of the penetration is higher than the grain size of the microcystalline and polysilicon solar cell indicated in Table 1. Consequently, the radio wave attenuation in these grains is very low.

3.3. Effect of the Grain Boundary Recombination Velocity. The curves of the penetration length of the radio waves for various recombination velocities at grain boundaries in the short circuit and open circuit are shown in Figures 3(a) and 3(b).

The curves in Figures 3 and 2 have, respectively, similar shapes; however, the values of the characteristic length of the penetration in Figure 3 are smaller than those in Figure 2.

In the short circuit, Figure 3(a), the characteristic length of the penetration increases slightly when the recombination velocity at grain boundaries increases. But this increase in the characteristic length of the penetration becomes more important in the open circuit condition (Figure 3(b)). In fact, an increase in the recombination velocity at grain boundaries corresponds to a decrease in the density of electrons

Table 1: Classification of the grain size.

Crystalline type	Microcrystalline	Polycrystalline	Multicrystalline	Single crystalline
Symbol	μc-Si	Pc-Si	Mc-Si	Sc-Si
Grain size	$g_x \leq 1\,\mu$m	$1\,\mu\text{m} \leq g_x \leq 1$ mm	$1\text{ mm} \leq g_x \leq 10$ cm	$g_x \geq 10$ cm

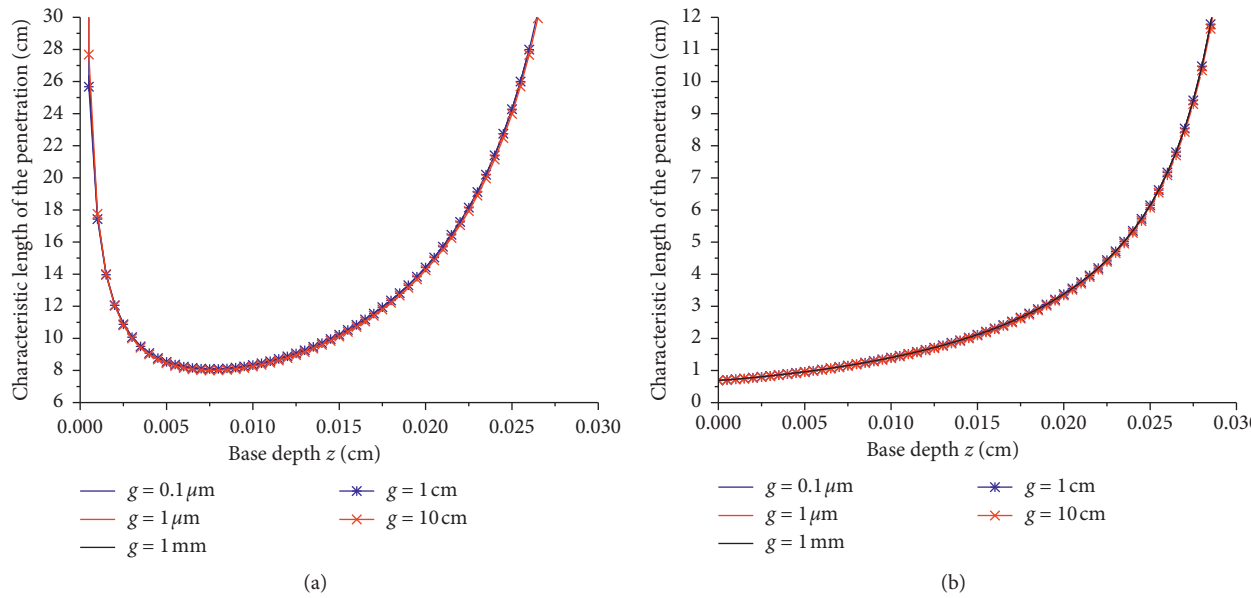

Figure 2: Characteristic length of the penetration against base depth for different grain sizes in (a) short circuit and (b) open circuit ($S_{gb} = 10^3$ cm s^{-1}).

Table 2: Behaviour of radio waves in the vicinity of the junction in the short circuit.

Crystalline type	Microcrystalline	Polycrystalline	Multicrystalline	Single crystalline
Grain size	$g_x \leq 1\,\mu$m	$1\,\mu\text{m} \leq g_x \leq 1$ mm	$1\text{ mm} \leq g_x \leq 10$ cm	$g_x \geq 10$ cm
Comparison between l_p and g	$l_p \gg g$	$l_p \gg g$	$l_p > g$	$l_p \simeq g$
Behaviour of the radio wave	Attenuation rate inferior to 5.56×10^{-4}%	Attenuation rate inferior to 0.55%	Attenuation rate inferior to 63.3%	Attenuation rate equal to 63.3%

Table 3: Behaviour of radio waves inside the base of the polysilicon grain in the short circuit.

Crystalline type	Microcrystalline	Polycrystalline	Multicrystalline	Single crystalline
Grain size	$g_x \leq 1\,\mu$m	$1\,\mu\text{m} \leq g_x \leq 1$ mm	$1\text{ mm} \leq g_x \leq 10$ cm	$g_x \geq 10$ cm
Comparison between l_p and g	$l_p \gg g$	$l_p \gg g$	$l_p \geq g$	$l_p \simeq g$
Behaviour of the radio wave	Attenuation rate inferior to 10^{-3}%	Attenuation rate inferior to 1%	Attenuation rate inferior to 63.3%	Attenuation rate equal to 63.3%

photogenerated and consequently to an increase in the penetration length.

As in the previous paragraph, one can conclude that the radio wave attenuation in the microcystalline and polysilicon grain is very low.

3.4. Attenuation Factor of Radio Waves. The analysis of the behaviour of the attenuation factor is another way to investigate the propagation of radio waves into the polysilicon grain. This was done considering the variable x to be equal to the grain size g_x and considering also the grain size and the recombination velocity at grain boundaries.

The analysis was conducted taking cognizance that when the value of the attenuation factor approaches unity ($\exp(-g_x/l_p) \longrightarrow 1$), the radio waves propagate into the grain with a negligible attenuation. In this case, the polysilicon grain behaves like an insulator (electric conductivity approaches zero). In the opposite case, when the value of the

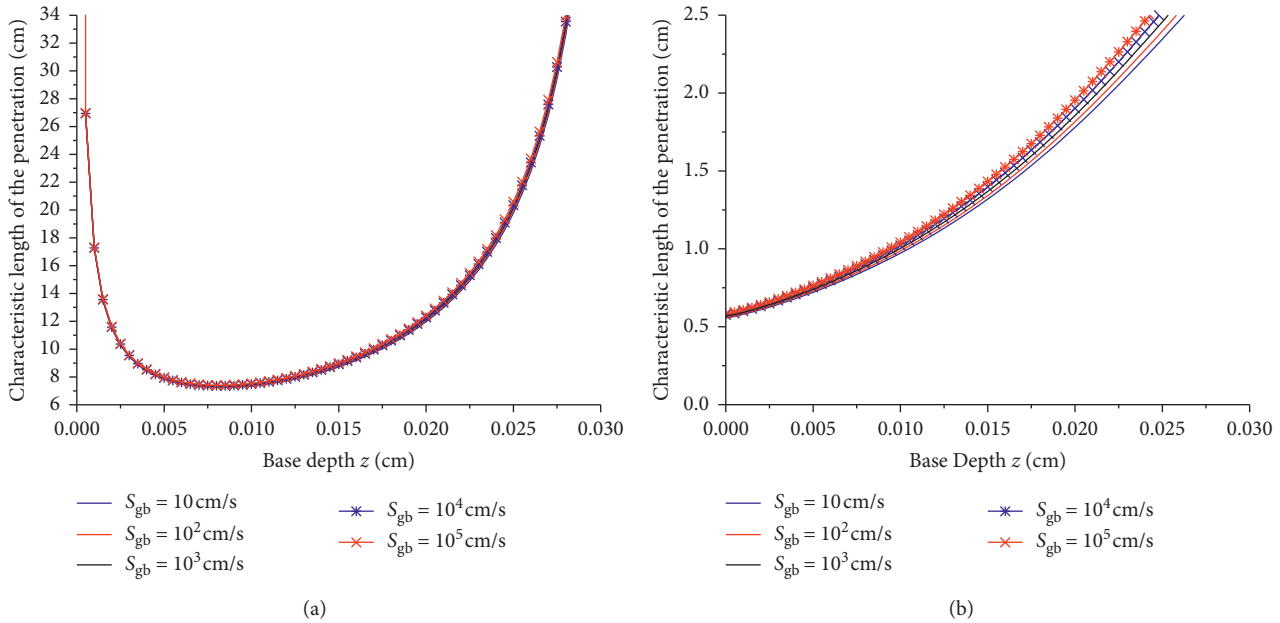

FIGURE 3: Characteristic length of the penetration versus base depth for different grain boundary recombination velocity in the short circuit (a) and open circuit (b) ($g = g_x = g_y = 0.01$ cm).

attenuation factor approaches zero ($\exp(-g_x/l_p) \longrightarrow 0$), the radio waves vanish in the grain. So the polycrystalline silicon grain behaves like an electric conductor (electric conductivity assuming higher value).

3.5. Effect of the Grain Size. Figures 4(a) and 4(b) plot the attenuation factor of the electromagnetic wave against the base depth for different grain sizes of silicon solar cells in short circuit and open circuit conditions.

As in the case of Figure 2(a), Figure 4(a) shows three characteristics regions: the attenuation factor decreases in the first region close to the junction where the quantity of excess minority carriers photogenerated increases with the base depth [7–10]. Then, the attenuation factor is constant with the lowest value in the second region inside the base where the quantity of excess minority carriers photogenerated is maximum [7–10]. At last, the attenuation factor increases in the third region where the quantity of electrons photogenerated decreases with the base depth [7–9]. Indeed, the increase in the photogeneration of electrons leads to an increase in the electric conductivity of the polycrystalline silicon grain which becomes a more and more electric conductor leading to an increase in the wave attenuation so there is a decrease in the attenuation factor. The lowest value of the attenuation factor is about 0.9408 (for $z = 0.0075$ cm), for the grain size $g = 10$ cm, leading to an attenuation of radio waves and an attenuation rate of about 5.92%. One can conclude that the attenuation of radio waves is negligible.

In the open circuit, curves in Figure 4(b) show that the attenuation factor increases from the junction to the back side of the polysilicon grain resulting in a decrease in the attenuation of radio waves. Indeed, in the open circuit, the quantity of electrons photogenerated decreases from the junction to the back side of the polysilicon grain [7–9] resulting in a decrease in its electric conductivity. When the electric conductivity of the polycrystalline silicon grain decreases, the grain behaves more and more like an insulator and the attenuation factor increases to reach its maximum value which is one. In this case; the attenuation of radio waves decreases. When the grain size increases, the attenuation factor decreases to reach its minimum value which is 0.4932 at the junction for the grain size $g = 10$ cm, resulting in an attenuation rate of 50.68%. But for the grain size $g = 1$ cm corresponding to a polycrystalline silicon grain, the attenuation factor at the junction is 0.925 and the attenuation rate is 7.5%.

The quantity of carriers photogenerated in the open circuit is higher than the one of the short circuit, so the electric conductivity of the solar cell in the open circuit is higher than the one of the short circuit. As the operating point of a solar cell lies between the short circuit and the open circuit, the radio wave attenuation is negligible for microcrystalline, polycrystalline, and multicrystalline silicon grains.

In the next lines, the radio wave evolution while the recombination velocity at grain boundaries varies is analyzed.

3.6. Effect of the Grain Boundary Recombination Velocity. The curves of radio wave attenuation factor in a polycrystalline silicon grain for various recombination velocities at grain boundaries in the short circuit and the open circuit are shown in Figures 5(a) and 5(b).

The curves in Figures 5 and 4 have, respectively, similar shapes. In the short circuit, Figure 5(a), the attenuation factor increases when the recombination velocity at grain

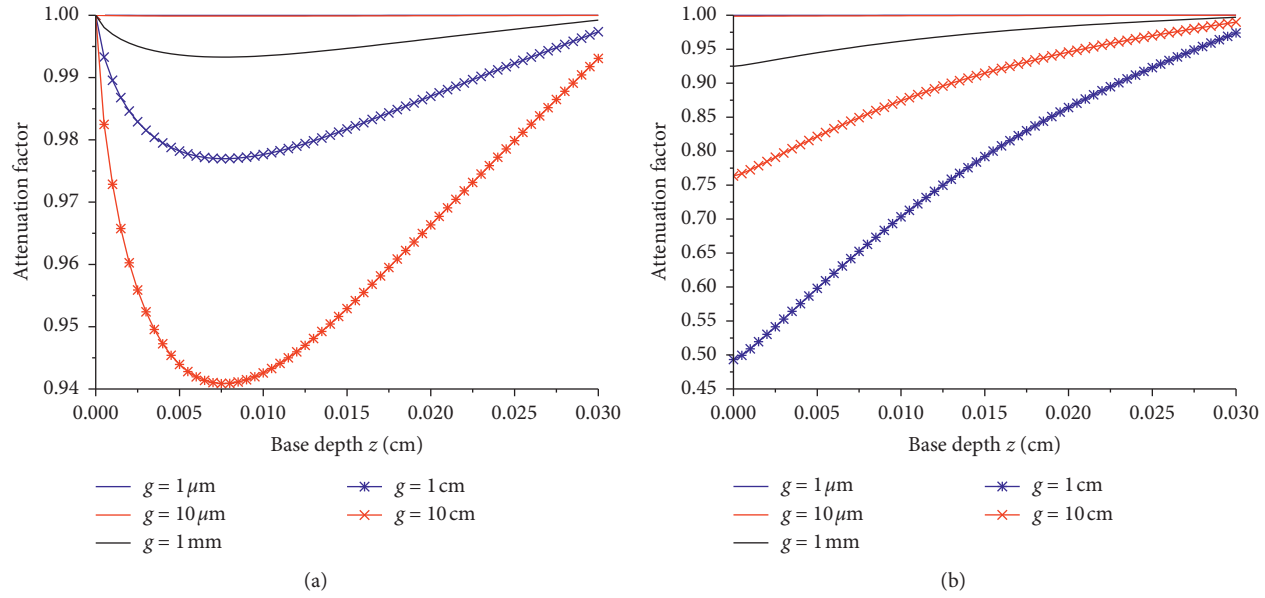

Figure 4: Attenuation factor of radio wave versus base depth for different grain sizes in short circuit (a) and open circuit (b) ($S_{gb} = 10^3$ cm s^{-1}).

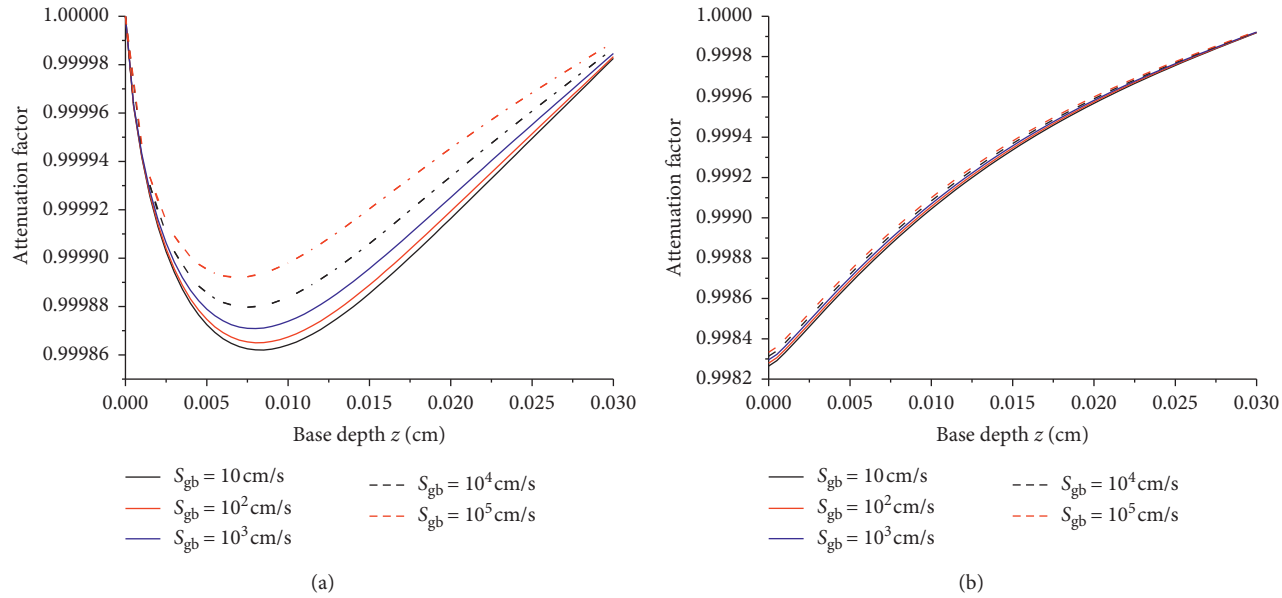

Figure 5: Attenuation factor of the electromagnetic wave versus base depth for different grain boundary recombination velocity in short circuit (a) and open circuit (b) ($g = g_x = g_y = 0.01$ cm).

boundaries increases also while in the open circuit (Figure 5(b)), the attenuation factor increases slightly with the increase in the grain boundary recombination velocity.

The increase in the grain boundary recombination velocity leads to a decrease in the number of the photogenerated electrons in the base of the polysilicon grain and consequently a decrease in its electric conductivity. The decrease in the electric conductivity of the polycrystalline silicon grain leads to an increase in the attenuation factor since the polycrystalline silicon grain behaves more and more like an insulator. The consequence is the decrease in radio wave attenuation.

In the short circuit, the minimum value of the attenuation factor is 0.99986 resulting in an attenuation rate of 0.014% while in the open circuit, the minimum value of the attenuation factor, at the junction, is 0.99826 leading to an attenuation rate of 0.174%. These values are negligible and, consequently, the effect of grain boundary recombination velocity on the attenuation factor of a polysilicon grain can be neglected.

As in the previous work [1], we can conclude that radio wave attenuation in the polysilicon grain is negligible; accordingly, the attenuation factor is taken to be equal to unity. The final forms of equations (3) and (4), in real notation, give the final expressions of electric and magnetic fields into the polysilicon grain: these final expressions of electric and magnetic fields are given by equations (6) and (7) as follows:

$$\overrightarrow{E}(x,t) = E_0 \overrightarrow{e}_z \cos(\omega\sqrt{\varepsilon\mu}\, x - \omega t), \tag{6}$$

$$\overrightarrow{B}(x,t) = -\frac{E_0\sqrt{\mu_r\varepsilon_r}}{c}\overrightarrow{e}_y \cos(\omega\sqrt{\mu\varepsilon}\, x - \omega t). \tag{7}$$

4. Conclusions

Modelling and simulation of the propagation of radio waves into the base of a polysilicon grain illuminated by the multispectral light was studied. Based on the expressions of the electric and magnetic fields into the grain, the study showed that the attenuation of the electromagnetic field is negligible so that the attenuation factor can be assumed equal to unity. The new expressions of the electric and magnetic fields into the polysilicon grain will be used later to solve the magneto-transport equation and the continuity equation of electrons in order to study the performance of a polysilicon grain under the electromagnetic wave generated by radio antennas.

Data Availability

The data used to support the findings of this study are available from the corresponding author upon request.

Conflicts of Interest

The authors declare that there are no conflicts of interest regarding the publication of this paper.

Acknowledgments

The authors are grateful to the International Science Program (ISP) for supporting their research group (energy and environment).

References

[1] A. Ouedraogo, V. d. D. B. Barandja, I. Zerbo, M. Zoungrana, E. W. Ramde, and D. J. Bathiebo, "A theoretical study of radio wave attenuation through a polycrystalline silicon solar cell," *Turkish Journal of Physics*, vol. 41, no. 4, pp. 314–325, 2017.

[2] J. Dugas, "3D modelling of a reverse cell made with improved multicrystalline silicon wafers," *Solar Energy Materials and Solar Cells*, vol. 32, no. 1, pp. 71–88, 1994.

[3] B. Ba and M. Kane, "Open-circuit voltage decay in polycrystalline silicon solar cells," *Solar Energy Materials and Solar Cells*, vol. 37, no. 3-4, pp. 259–271, 1995.

[4] K. Misiakos, C. H. Wang, A. Neugroschel, and F. A. Lindholm, "Simultaneous extraction of minority-carrier transport parameters in crystalline semiconductors by lateral photocurrent," *Journal of Applied Physics*, vol. 67, no. 1, pp. 321–333, 1990.

[5] I. Zerbo, M. Zoungrana, A. Seré, and F. Zougmoré, "Silicon solar cell under electromagnetic wave in steady state: effect of the telecommunication source's power of radiation," *IOP Conference Series: Materials Science and Engineering*, vol. 29, Article ID 012019, 2012.

[6] P. A. Bassore, "Defining terms for crystalline silicon solar cells," *Progress in Photovoltaics: Research and Applications*, vol. 2, pp. 177–179, 1994.

[7] M. Zoungrana, I. Zerbo, A. Seré, B. Zouma, and F. Zougmore, "3D study of bifacial silicon solar cell under intense light concentration and under external constant magnetic field," *Global Journal of Engineering Research*, vol. 10, no. 1-2, pp. 113–124, 2011.

[8] M. Zoungrana, B. Dieng, O. H. Lemrabott et al., "External electric field influence on charge carriers and electrical parameters of polycrystalline silicon solar cell," *Research Journal of Applied Sciences, Engineering and Technology*, vol. 4, no. 17, pp. 2967–2972, 2012.

[9] I. Diatta, I. Ly, M. Wade, M. S. Diouf, S. Mbodji, and G. Sissoko, "Temperature effect on capacitance of a silicon solar cell under constant white biased light," *World Journal of Condensed Matter Physics*, vol. 6, no. 3, pp. 261–268, 2016.

[10] H. L. Diallo, A. Seïdou Maiga, A. Wereme, and G. Sissoko, "New approach of both junction and back surface recombination velocities in a 3D modelling study of a polycrystalline silicon solar cell," *The European Physical Journal Applied Physics*, vol. 42, no. 3, pp. 203–211, 2008.